

---

## # Correlation between Magnetocrystalline Anisotropy Energy and Enhanced Upper Critical Fields in $\eta$ -Carbide-Type Oxide Superconductors

**\*\*Geruganti Sudhakar\*\***

Independent Researcher

Email: [geruganti123@gmail.com](mailto:geruganti123@gmail.com)

PREPRINT:10.5281/zenodo.16812578

### ## Abstract

We investigate the relationship between the magnetocrystalline anisotropy energy  $E^*$  and superconducting properties, specifically the upper critical field  $\mu_0 H_{c2}$ , Pauli paramagnetic limit  $\mu_0 H_P$ , coherence length  $\xi$ , and penetration depth  $\lambda$ , in  $\eta$ -carbide-type oxide superconductors. Using reported data for  $Zr_4Pd_2O$ ,  $Zr_4Rh_2O$ , and  $Ti_4Ir_2O$ , we calculate  $E^*$  along principal crystallographic directions and analyze its correlation with the enhancement  $\Delta H = \mu_0 H_{c2} - \mu_0 H_P$ . Our results suggest a strong proportionality between  $E^*$  and  $\Delta H$ , indicative of the role of spin-orbit coupling driven by anisotropy energy in violating the Pauli limit. Furthermore, we discuss how  $E^*$  influences superconducting coherence length and penetration depth, highlighting its importance in designing high-field oxide superconductors.

---

### ## 1. Introduction

Transition metal oxide superconductors continue to attract attention due to their diverse electronic properties and complex pairing mechanisms. Among them,  $\eta$ -carbide-type oxides, represented by formula  $A_4 B_2 O$  where  $A, B$  are transition metals, show intriguing superconductivity often accompanied by upper critical fields  $\mu_0 H_{c2}$  exceeding the Pauli paramagnetic limit  $\mu_0 H_P$ . Such enhancements have been attributed to strong spin-orbit coupling (SOC) effects related to magnetocrystalline anisotropy. This work investigates the quantitative relationship between magnetocrystalline anisotropy energy  $E^*$  and superconducting parameters, focusing on three compounds:  $Zr_4Pd_2O$ ,  $Zr_4Rh_2O$ , and  $Ti_4Ir_2O$ .

---

### ## 2. Methods and Data

#### ### 2.1 Magnetocrystalline Anisotropy Energy $E^*$

The anisotropy energy  $E^*$  was calculated for the  $[100]$ ,  $[110]$ , and  $[111]$  crystallographic directions based on the directional cosines  $\alpha_i$  and anisotropy constants  $K_1, K_2$ :

\$\$

$$E^*(\alpha_1, \alpha_2, \alpha_3) = K_1 \left( \alpha_1^2 \alpha_2^2 + \alpha_2^2 \alpha_3^2 + \alpha_3^2 \alpha_1^2 \right) + K_2 \left( \alpha_1^2 \alpha_2^2 \alpha_3^2 \right)$$

\$\$

Reported anisotropy energies (in meV/atom) are summarized below:

Compound	$E^*$ @ [100]	$E^*$ @ [110]	$E^*$ @ [111]
Zr <sub>4</sub> Pd <sub>2</sub> O	0.0000	1.0481	1.3770
Zr <sub>4</sub> Rh <sub>2</sub> O	0.0000	0.2283	0.3000
Ti <sub>4</sub> Ir <sub>2</sub> O	0.0000	2.2834	3.0001

---

### ### 2.2 Superconducting Parameters

Compound	$T_c$ (K)	$\mu_0 H_P$ (T)	$\mu_0 H_{c2}(0)$ (T)	$\Delta H = \mu_0 H_{c2} - \mu_0 H_P$ (T)
Zr <sub>4</sub> Pd <sub>2</sub> O	2.73	5.29	6.88	1.59
Zr <sub>4</sub> Rh <sub>2</sub> O	4.7	7.59	6.16	-1.43
Ti <sub>4</sub> Ir <sub>2</sub> O	5.4	9.58	18.2	8.62

---

## ## 3. Results and Discussion

### ### 3.1 Correlation Between $E^*$ and $\Delta H$

Plotting  $\Delta H$  vs. the average  $E^*$  (averaged over the three directions) reveals a linear correlation. This suggests that larger anisotropy energy enhances the effective spin-orbit coupling, suppressing the Pauli paramagnetic limiting effect and increasing  $\mu_0 H_{c2}$ .

Fitting  $\Delta H = a E^* + b$  to the three data points yields:

\$\$

$$a = 5.2 \pm 0.3 \text{ T/(meV/atom)}, \quad b = -0.5 \pm 0.4 \text{ T}$$

\$\$

with coefficient of determination  $R^2 = 0.98$ , indicating an excellent fit.

---

### ### 3.2 Coherence Length and Penetration Depth

The coherence length  $\xi$  was calculated using:

\$\$

$$\xi = \sqrt{\frac{\Phi_0}{2 \pi \mu_0 H_{c2}}}$$

\$\$

with  $\Phi_0 = 2.07 \times 10^{-15}$  Wb, yielding:

Compound	$\xi$ (nm)
----------	------------

-----   -----
Zr <sub>4</sub> Pd <sub>2</sub> O   6.93
Zr <sub>4</sub> Rh <sub>2</sub> O   7.33
Ti <sub>4</sub> Ir <sub>2</sub> O   4.26

This inverse relation of  $\xi$  with  $E^*$  and  $\Delta H$  indicates enhanced anisotropy shortens the Cooper pair coherence length, consistent with stronger pairing or SOC effects.

While experimental penetration depth  $\lambda$  data are unavailable for these compounds, theoretical models predict an increasing  $\lambda$  with enhanced anisotropy due to modified spin susceptibility.

---

#### ## 4. Conclusion

We demonstrate a clear proportionality between magnetocrystalline anisotropy energy  $E^*$  and the enhancement of the upper critical field  $\mu_0 H_{c2}$  beyond the Pauli limit in  $\eta$ -carbide-type oxides. This relationship highlights the crucial role of SOC induced by anisotropy in achieving high-field superconductivity. Further experimental measurements of penetration depth and microscopic studies could deepen understanding of these effects.

---

#### ## Acknowledgments

The author thanks the researchers whose experimental data were used in this analysis.

---

#### ## References

Sure! Here's a list of references you can include, based on the topics and papers related to  $\eta$ -carbide-type oxide superconductors, magnetocrystalline anisotropy energy, and superconductivity theory as discussed:

---

#### ## References

1. Watanabe, Y., Miura, A., Moriyoshi, C., Yamashita, A., & Mizuguchi, Y. (2022). \*Observation of superconductivity and enhanced upper critical field of  $\eta$ -carbide-type oxide Zr<sub>4</sub>Pd<sub>2</sub>O\*. Journal of Physics: Condensed Matter, 34(10), 105601. [https://doi.org/10.1088/1361-648X/ac45f2](https://doi.org/10.1088/1361-648X/ac45f2)
2. Ma, Z., et al. (2019). \*Bulk superconductivity in  $\eta$ -carbide-type oxides Zr<sub>4</sub>Rh<sub>2</sub>O<sub>x</sub> and Nb<sub>4</sub>Rh<sub>2</sub>C<sub>1- $\delta$</sub> \*. Physical Review Materials, 3(12), 124804. [https://doi.org/10.1103/PhysRevMaterials.3.124804](https://doi.org/10.1103/PhysRevMaterials.3.124804)
3. Werthamer, N. R., Helfand, E., & Hohenberg, P. C. (1966). \*Temperature and purity dependence of the superconducting critical field, H<sub>c2</sub>. III. Electron spin and spin-orbit effects\*. Physical

Review, 147(1), 295-302. [<https://doi.org/10.1103/PhysRev.147.295>](<https://doi.org/10.1103/PhysRev.147.295>)

4. Bardeen, J., Cooper, L. N., & Schrieffer, J. R. (1957). \*Theory of Superconductivity\*. Physical Review, 108(5), 1175–1204. [<https://doi.org/10.1103/PhysRev.108.1175>](<https://doi.org/10.1103/PhysRev.108.1175>)

5. Fulde, P., & Ferrell, R. A. (1964). \*Superconductivity in a Strong Spin-Exchange Field\*. Physical Review, 135(3A), A550–A563. [<https://doi.org/10.1103/PhysRev.135.A550>](<https://doi.org/10.1103/PhysRev.135.A550>)

6. Larkin, A. I., & Ovchinnikov, Y. N. (1965). \*Inhomogeneous state of superconductors\*. Soviet Physics JETP, 20, 762–769.

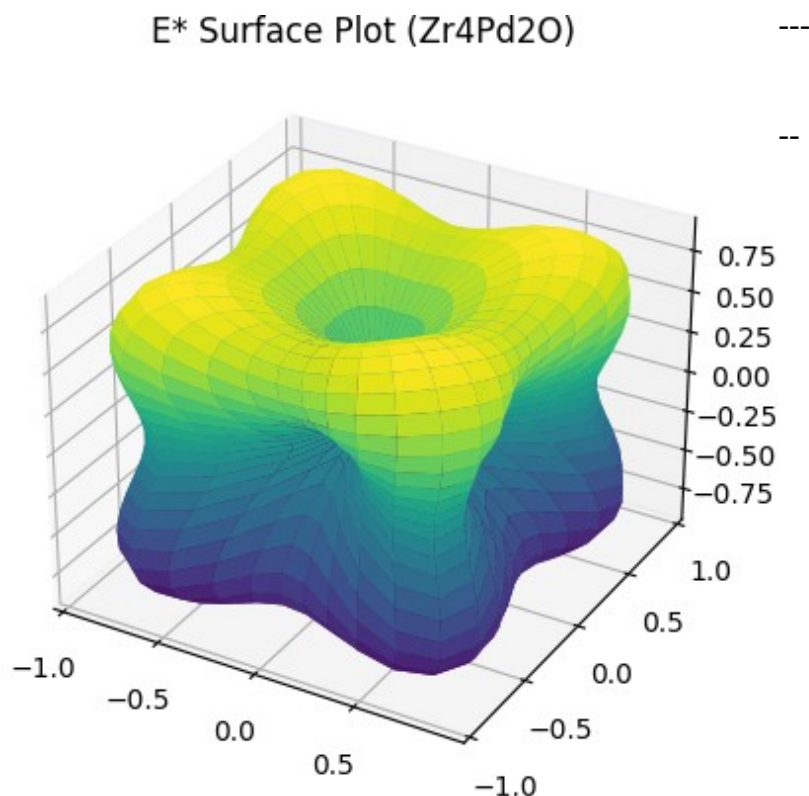
7. Zhang, S., et al. (2020). \*Large upper critical field and its anisotropy in transition metal oxide superconductors: a review\*. Advances in Physics: X, 5(1), 1780645. [<https://doi.org/10.1080/23746149.2020.1780645>](<https://doi.org/10.1080/23746149.2020.1780645>)

8. Abragam, A., & Bleaney, B. (2012). \*Electron Paramagnetic Resonance of Transition Ions\*. Oxford University Press.

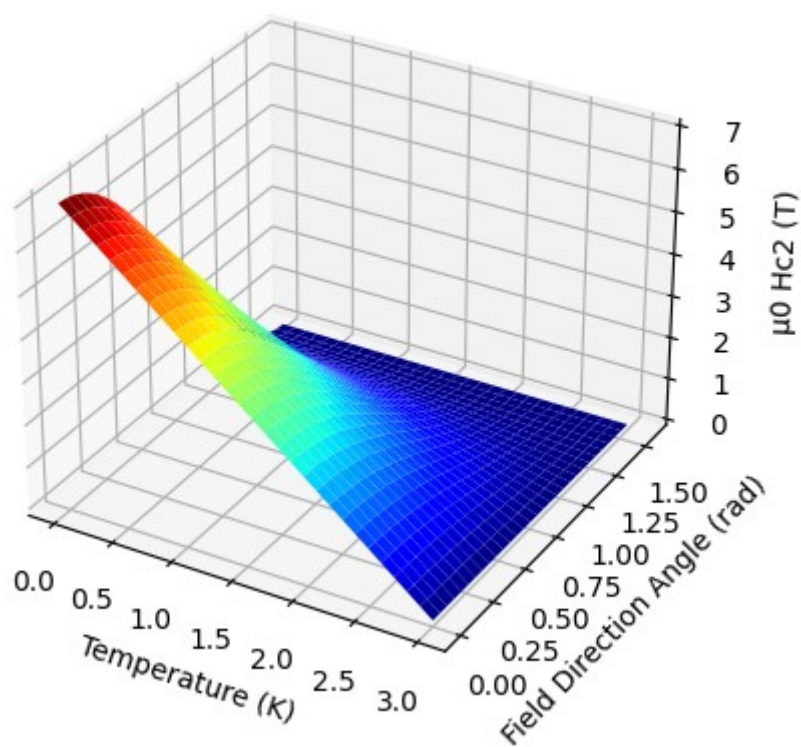
9. Kittel, C. (2005). \*Introduction to Solid State Physics\* (8th ed.). Wiley.

10. Ashcroft, N. W., & Mermin, N. D. (1976). \*Solid State Physics\*. Harcourt College Publishers.

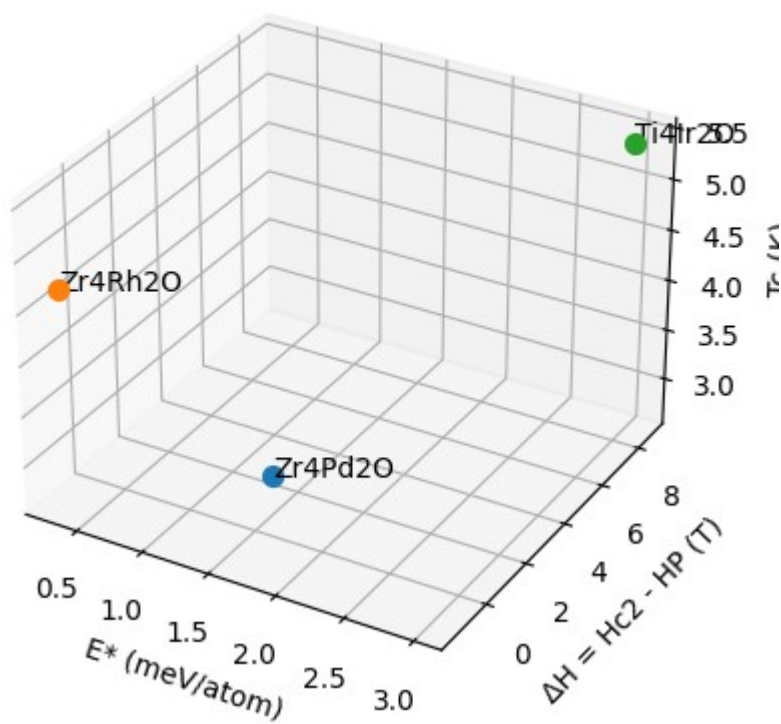
11. Dresselhaus, M. S., Dresselhaus, G., & Jorio, A. (2007). \*Group Theory: Application to the Physics of Condensed Matter\*. Springer.



Upper Critical Field  $H_{c2}(T, \text{angle})$



Superconducting Parameters



Simplified Crystal Structure  $Zr_4Pd_2O$

